Physics and Imaging in Radiation Oncology 16 (2020) 134–137

Contents lists available at ScienceDirect

Physics and Imaging in Radiation Oncology

journal homepage: www.sciencedirect.com/journal/physics-and-imaging-in-radiation-oncology

Short Communication

Dose-response of deformable radiochromic dosimeters for spot scanning proton therapy

Simon V. Jensen [a,*], Lia B. Valdetaro [a], Per R. Poulsen [a], Peter Balling [b], Jørgen B.B. Petersen [a], Ludvig P. Muren [a,1]

[a] Danish Center for Particle Therapy, Aarhus University Hospital, Aarhus, Denmark
[b] Department of Physics and Astronomy, Aarhus University, Aarhus, Denmark

ARTICLE INFO

Keywords:
Proton therapy
Deformation
3D dosimetry
Monte Carlo

ABSTRACT

Intrafractional motion and deformation influence proton therapy delivery for tumours in the thorax, abdomen and pelvis. This study aimed to test the dose–response of a compressively strained three-dimensional silicone-based radiochromic dosimeter during proton beam delivery. The dosimeter was read-out in its relaxed state using optical computed tomography and calibrated for the linear energy transfer, based on Monte Carlo simulations. A three-dimensional gamma analysis showed a 99.3% pass rate for 3%/3 mm and 93.9% for 2%/2 mm, for five superimposed measurements using deformation-including Monte Carlo dose calculations as reference. We conclude that the dosimeter's dose–response is unaffected by deformations.

1. Introduction

Intrafractional motion, e.g. due to respiration, circulation, or peristalsis, influences proton therapy delivery to tumour sites particularly in the thorax, abdomen, and pelvis. Organ motion and deformation vary in complexity depending on the region of interest. Regions near the lung are dealt with using e.g. breath-hold techniques in combination with image based monitoring [1], while approaches such as respiratory gating and tumour tracking are also being explored [2–5].

Independent of the motion management strategy used to account for motion and deformations, it is important to experimentally verify its performance. In a photon-based study Ehrbar *et al.* [6] developed a dynamical abdominal phantom which could deform a liver insert. During the delivery of photon beams, radiochromic films and scintillators were applied to measure the dose-deposition for real-time motion-adaptive radiotherapy. Scintillators and radiochromic films have been found to be applicable also for proton irradiation [7–9]. Scintillators can provide real-time point measurements, but the limited spatial information makes a three-dimensional (3D) comparison between the deformed and undeformed phantom difficult. A deformable 3D dosimeter would give the special information necessary to evaluate the influence of deformation and motion during irradiation and might prove valuable for protocol- or patient-specific dose verification in these regions [10].

A previously developed silicone-based 3D radiochromic dosimeter has been shown to behave as an incompressible hyperelastic deformable material [11]. Under a strain down to 60% of its undeformed length, the volume of the dosimeter remained constant, exhibiting an average volume change below 2%. The silicone-based radiochromic dosimeter has a linear dose–response that was found to be dose-rate independent up to 6 Gy,min^{-1} when irradiated using a photon beam [12–14]. The dose–response is defined as the change in optical density in a voxel that is irradiated with a certain dose. The dosimeter's dose–response to proton beams has also been studied [15], showing that a linear energy transfer (LET) dependent calibration was required to translate the change in optical density to dose [16,17].

The aim of this study was to test whether the dose–response of a silicone-based dosimeter changed during deformation when irradiated with protons and to benchmark the measured dose distributions against Monte Carlo (MC) simulations.

* Corresponding author at: Danish Center for Particle Therapy, Aarhus University Hospital, Office B420, Palle Juul Jensens Blvd. 35, 8200 Aarhus N, Denmark.
E-mail address: sivije@au.dk (S.V. Jensen).

[1] Dr. Ludvig Muren, a co-author of this paper, is an Editor-in-Chief of Physics & Imaging in Radiation Oncology. The editorial process for this manuscript was managed independently from Dr. Muren and the manuscript was subject to the Journal's usual peer-review process.

https://doi.org/10.1016/j.phro.2020.11.004
Received 6 July 2020; Received in revised form 3 November 2020; Accepted 10 November 2020
Available online 20 November 2020

2. Materials and methods

2.1. Dosimeter fabrication

Five dosimeters were cast from the same batch, containing 93.1 wt% silicone elastomer and 5.1 wt% curing agent both from a SYLGARD® 184 silicone elastomer kit (Dow Corning), as well as 1.5 wt% chloroform (Sigma-Aldrich), and 0.26 wt% leucomalachite green (LMG) dye.

The silicone elastomer was added to a solution of LMG and chloroform and mixed thoroughly. Subsequently, the curing agent was added, and it was mixed again. The mixture was vacuum desiccated to remove residual air bubbles.

Once degassed, the mixture was poured into cylindrical acrylic-glass moulds with aluminium bottoms equipped with an O-ring. The inner diameter of the moulds was 50 mm and the height was 50 mm. The dosimeters were then left to cure for 72 h. To separate the dosimeters from their moulds, a vacuum pump was attached on one end of a dosimeter, which forced the dosimeter to be released from the mould.

2.2. Pre- and post-irradiation optical read-out

Optical computed tomography (OCT) read-outs were performed two hours before and one hour after irradiation. To avoid refraction effects during read-out, the dosimeters were immersed in a refractive-index-matching liquid, consisting of demineralized water and glycerol. One thousand 2D projections at different angles were captured with a Vista 16 (Modus Medical Devices Inc.) OCT scanner for each dosimeter read-out. The projections were used for reconstructing the 3D optical density distribution with the Feldkamp-Davis-Kress (FDK) algorithm [18] to achieve a spatial resolution of 1 mm^3 voxels. The dosimeters were read-out in their relaxed state.

2.3. Deformation and irradiation

During irradiation, the dosimeters were compressively strained along the length axis from 50 mm to 30 mm in steps of 5 mm between two square acrylic-glass plates. The acrylic plates were 10 mm thick and their side length was 120 mm. The two plates were connected using four bolts, which ensured an equally distributed pressure. The dosimeter stayed approximately cylindrical during deformation.

One dosimeter was used for each deformation step and irradiated through the centre of one of the end surfaces with a single 105 MeV proton pencil beam (84 mm range) from a Varian ProBeam cyclotron. A 50-mm-thick block of Solid Water® placed at the entrance side of the dosimeter ensured that the Bragg peak of the proton beam was located inside the dosimeter. A dose-rate of 20,000 MU/min was applied until reaching a water-equivalent dose of 12 Gy in the Bragg peak according to an Eclipse (Varian Medical Systems) calculation using the PCS 13.7 dose calculation algorithm. The five measurements were then superimposed to emulate the effect of the full deformation sequence.

2.4. Dose and linear energy transfer calculations

The experimental setup was simulated in the MC program Topas version 3.2 [19], applying proton beam parameters based on in-house beam calibrations. In the MC calculations, dose and dose-averaged LET (LET_d) were scored in 1 mm^3 voxels for 25 million protons for each deformation step inside the dosimeter.

To take the deformation of the dosimeter into account in the MC calculation, it was assumed that the dosimeter stayed perfectly cylindrical under deformation with a constant volume. From volume conservation, the cylinder radius changes as $r = r_0\sqrt{l_0/l}$, where r_0 and l_0 denote the radius and length without strain and r and l are the radius and length during deformation.

The measured signal quenched in high-LET regions [12,16]. A calibration model, based on other dosimeters than used in this study, was constructed by aligning the simulated dose and OCT distributions of monoenergetic proton pencil beams (95 MeV) with an intensity-based minimization. Only points within a 1 mm radius from the central axis were included, to minimize uncertainties on the beam penumbra parametrization [20]. The quenching correcting factor (QCF) was estimated as a function of LET_d by comparing the measured dose to the MC dose. The resulting curve was then used to calibrate the OCT map voxel-by-voxel, following,

$$OCT_{calibrated} = \frac{OCT}{QCF(LET_d)},$$

where the LET_d values are from the MC calculation. Further detail about the calibration method can be found in the paper by Valdetaro *et al.* [20].

2.5. Gamma analysis

To compare the LET-calibrated OCT measurements with the MC dose calculation, we used a 3D gamma analysis with 3%/3 mm and 2%/2 mm criteria [21]. All OCT and MC data were normalized to the maximum dose in the first dosimeter (50 mm) located in the Bragg peak plateau, for the data to be comparable. Only voxels in the central 30 mm of the dosimeters with dose above 10% of the maximum dose in the MC calculation were included in the gamma analysis. Gamma values below or equal to 1 passed the test while values above 1 failed.

3. Results

The MC calculation and LET-calibrated OCT measurement for the deformation steps (Fig. 1) showed that the proton beam penetrated further into the dosimeter when strained while the width of the beam at the Bragg peak became narrower. The 3%/3 mm 3D gamma analysis for each of the deformation steps starting from 50 mm to 30 mm passed between 90% and 98% of the voxels, while the 2%/ 2 mm passed between 83% and 95%. The largest deviations in the gamma analysis were at the edges of the proton beam.

The superimposed LET-calibrated measurements of the five dosimeters showed a smeared-out and elongated Bragg peak where the distal edge lost its distinct steep gradient compared to the undeformed case (Fig. 2). The 3%/3 mm 3D gamma analysis for the superimposed case passed 99.3% of the voxels, while the 2%/2 mm passed 93.9%.

4. Discussion

This paper investigated whether the dose–response of a deformable silicone-based radiochromic dosimeter changes while being compressively strained. It was found that the dose–response of this dosimeter was unaffected by deformations, showing its potential for deformation- and motion-inclusive dosimetry.

The doses and LET derived from the MC calculation played a large role in determining the precision of the gamma analysis. A small discrepancy in the proton beam parameters influences the calculated dose distribution. In the in-house beam-parameter calibration used for the MC calculations, the angular divergence was not parametrized and could be energy-dependent, which affects the width of the simulated dose [17,20]. This could potentially explain why the largest deviations in the gamma analysis were near the edges of the proton beam. Similarly, a beam-energy mismatch influenced the range of the proton beam, however, the mismatch between the requested beam-energy and actual energy were corrected for in the parametrization. For some voxels near the distal edge of the Bragg peak, the MC calculated LET had a much higher value than surrounding voxels, influencing the LET-calibrated OCT measurements adversely. Simulating more particles would reduce this effect, but presumably not remove it entirely. Furthermore, a few

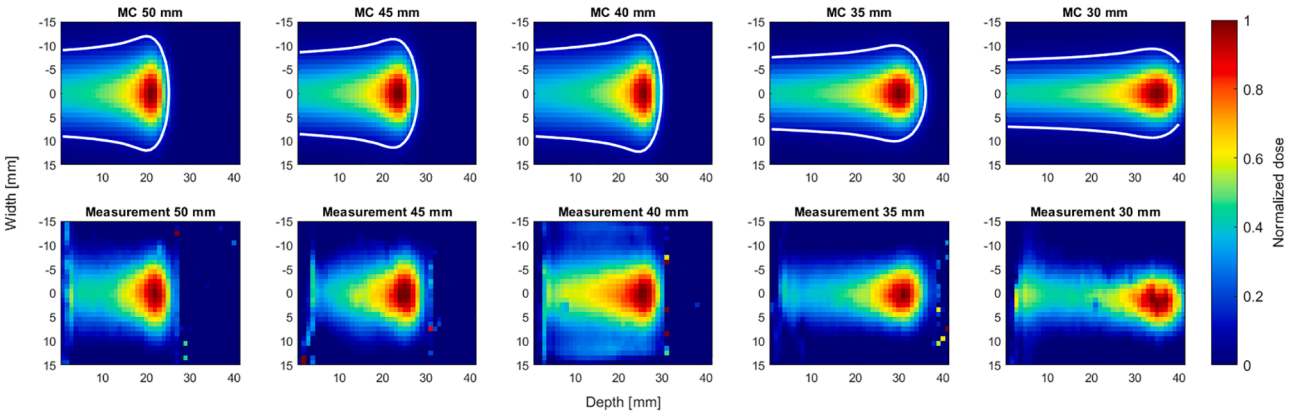

Fig. 1. The dose deposition in a section through the five dosimeters at the different strains indicated by the strained length above each image. The top row shows the MC calculations while the bottom row shows the LET-calibrated dose distributions in the dosimeter. An isocurve of 10% of the maximum dose is indicated by a white line. The 3%/3 mm 3D gamma analysis passed 96.1%, 94.3%, 93.7%, 98.5% and 90.3% of the voxels (left to right), while the 2%/2 mm passed 90.2%, 87.1%, 88.3%, 95.2% and 83.3%.

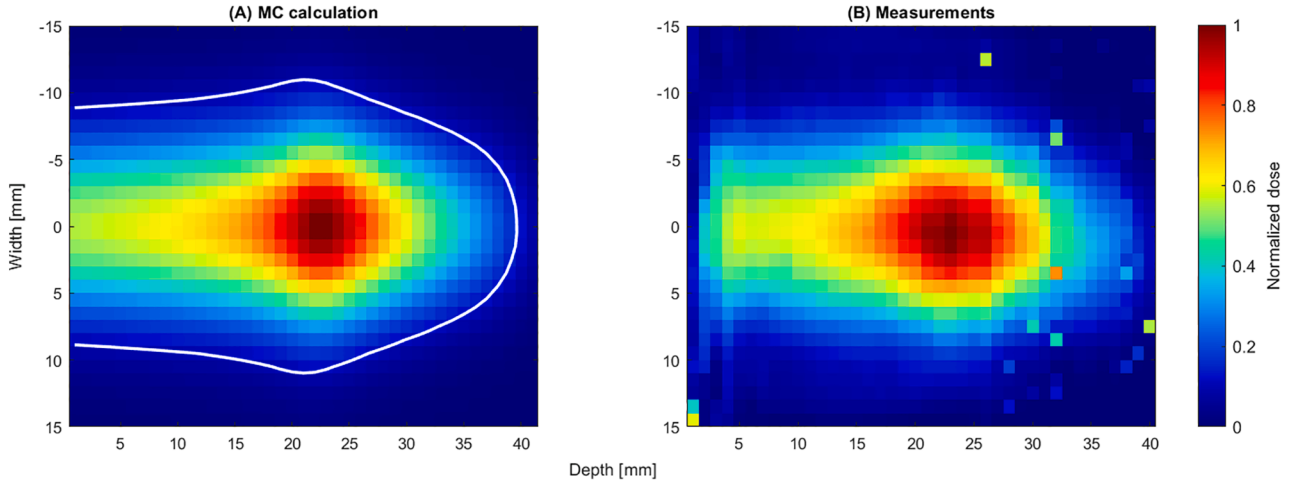

Fig. 2. The dose deposition in a section through the dosimeter from five superimposed proton spots delivered at deformations of 50 mm to 30 mm in steps of 5 mm. (A) Dose from MC calculation and (B) LET-calibrated dose distribution in the dosimeter. An isocurve of 10% of the maximum dose is indicated by a white line.

optical artefacts disturbed some of the OCT slices and in turn the gamma analysis. Finally, the reconstruction algorithm and the image alignment in the reconstruction played a large role in the data acquisition. If the reference scan and data scan were not exactly on top of each other, it would give an over- or under-response in the edges, which was also observed in our measurements. Fiducial markers in the dosimeters might improve image alignment.

The investigated dosimeters would be a great tool for testing patient-specific proton therapy delivery to anatomy that is prone to large deformations. However, performing an LET calibration is a labour-intensive task since every calibration requires a MC calculation of the LET map. Combined with the long curing time and non-reusability of the dosimeters, it might be challenging to introduce in a clinical workflow, on a patient-to-patient basis. Therefore, an analytical approach to account for the quenching would be ideal since in the current setup an incorrectly parametrized deformation would result in an incorrect LET calibration. Additionally, there might be a dose-rate dependence, which must be accounted for if proton-beam scanning should be used [20].

Maynard et. al. [22] used a N-isopropylacrylamide (NIPAM)-based gel dosimeter for photon dose measurements during deformations, combined with read-out using an x-ray CT scanner. As in this paper, their 3D dosimeter was compressively strained between two plates, where one was attached to a piston actuated by a stepper motor. However, they used wax beads as fiducial markers when performing deformable image registration (DIR) using the defDOSXYZnrc algorithm to calculate the warped dose. There is a large variety of DIR algorithms [23,24] and the choice of algorithm can affect the result. The results for a 3%/3 mm gamma analysis was a 95% pass-rate for the undeformed scenario and a 66% pass-rate for their DIR dose calculation for the deformed scenario. Our dosimeter performs as well as the NIPAM dosimeter when it is deformed and works for photon and proton beams. Furthermore, it does not need to be sealed in a latex container and can be moulded into arbitrary shapes.

To the best of our knowledge, this is the first study of 3D dosimetry in proton therapy focusing on deformations. It would be interesting to investigate the effects of respiration by deforming the dosimeters during irradiation as if being subjected to a breathing cycle during a proton beam delivery. In such future studies, it will be important to ensure that the size of the dosimeters does not prohibit read-out by attenuating the light in the OCT scanner beyond its sensitivity and that any dose-rate dependency is addressed. Furthermore, it would be interesting to incorporate fiducial markers such as Maynard et al. [22] and perform x-ray CT scans to verify how the dosimeter is deformed. To truly unlock the potential of 3D dosimeters, the dosimeters should be cast into anthropomorphic shapes and deformed as they would be in a body.

In conclusion, we have found that the dose–response of a silicone-based radiochromic dosimeter was unaffected by deformations, based on the high gamma pass rate not only for the individual dosimeters but

also for five superimposed measurements. The dosimeters are suitable for 3D motion-inclusive dose measurements in proton therapy.

Declaration of Competing Interest

The authors declare that they have no known competing financial interests or personal relationships that could have appeared to influence the work reported in this paper.

Acknowledgements

This research project was supported by the Novo Nordisk Foundation.

A special thanks to Mateusz Sitarz, Peter Skyt and Christian Søndergaard for assistance with proton irradiations. Thanks to Janus Kramer Møller for initial help with the dosimeter preparations. Finally, thanks to DCPT proton Monte Carlo group for the MC beam model parameters.

References

[1] Boda-Heggemann J, Knopf A-C, Simeonova-Chergou A, Wertz H, Stieler F, Jahnke A, et al. Deep Inspiration Breath Hold—Based Radiation Therapy: A Clinical Review. Int J Radiat Oncol Biol Phys 2016;94(3):478–92. https://doi.org/10.1016/j.ijrobp.2015.11.049.

[2] Gelover E, Deisher AJ, Herman MG, Johnson JE, Kruse JJ, Tryggestad EJ. Clinical implementation of respiratory-gated spot-scanning proton therapy: An efficiency analysis of active motion management. J Appl Clin Med Phys 2019;20(5):99–108. https://doi.org/10.1002/acm2.12584.

[3] Shimizu S, Miyamoto N, Matsuura T, Fujii Y, Umezawa M, Umegaki K, et al. A Proton Beam Therapy System Dedicated to Spot-Scanning Increases Accuracy with Moving Tumors by Real-Time Imaging and Gating and Reduces Equipment Size. PLoS One 2014;9:e94971. https://doi.org/10.1371/journal.pone.0094971.

[4] Chang JY, Zhang X, Knopf A, Li H, Mori S, Dong L, et al. Consensus Guidelines for Implementing Pencil-Beam Scanning Proton Therapy for Thoracic Malignancies on Behalf of the PTCOG Thoracic and Lymphoma Subcommittee. Int J Radiat Oncol Biol Phys 2017;99(1):41–50. https://doi.org/10.1016/j.ijrobp.2017.05.014.

[5] Bertholet J, Knopf A, Eiben B, McClelland J, Grimwood A, Harris E, et al. Real-time intrafraction motion monitoring in external beam radiotherapy. Phys Med Biol 2019;64:15TR01.. https://doi.org/10.1088/1361-6560/ab2ba8.

[6] Ehrbar S, Jöhl A, Kühni M, Meboldt M, Ozkan Elsen E, Tanner C, et al. ELPHA: Dynamically deformable liver phantom for real-time motion-adaptive radiotherapy treatments. Med Phys 2019;46(2):839–50. https://doi.org/10.1002/mp.13359.

[7] Shen J, Allred BC, Robertson DG, Liu W, Sio TT, Remmes NB, et al. A novel and fast method for proton range verification using a step wedge and 2D scintillator. Med Phys 2017;44(9):4409–14. https://doi.org/10.1002/mp.12439.

[8] Almurayshid M, Helo Y, Kacperek A, Griffiths J, Hebden J, Gibson A. Quality assurance in proton beam therapy using a plastic scintillator and a commercially available digital camera. J Appl Clin Med Phys 2017;18(5):210–9. https://doi.org/10.1002/acm2.12143.

[9] Vatnitsky SM. Radiochromic film dosimetry for clinical proton beams. Appl Radiat Isot 1997;48(5):643–51. https://doi.org/10.1016/S0969-8043(97)00342-4.

[10] Kang Y, Shen J, Liu W, Taylor PA, Mehrens HS, Ding X, et al. Impact of planned dose reporting methods on Gamma pass rates for IROC lung and liver motion phantoms treated with pencil beam scanning protons. Radiat Oncol 2019;14(1). https://doi.org/10.1186/s13014-019-1316-y.

[11] Kaplan LP, Høye EM, Balling P, Muren LP, Petersen JBB, Poulsen PR, et al. Determining the mechanical properties of a radiochromic silicone-based 3D dosimeter. Phys Med Biol 2017;62:5612–22. https://doi.org/10.1088/1361-6560/aa70cd.

[12] Høye EM, Skyt PS, Yates ES, Muren LP, Petersen JBB, Balling P. A new dosimeter formulation for deformable 3D dose verification. J Phys Conf Ser 2015;573:012067. https://doi.org/10.1088/1742-6596/573/1/012067.

[13] Høye EM, Balling P, Yates ES, Muren LP, Petersen JBB, Skyt PS. Eliminating the dose-rate effect in a radiochromic silicone-based 3D dosimeter. Phys Med Biol 2015;60(14):5557–70. https://doi.org/10.1088/0031-9155/60/14/5557.

[14] De Deene Y, Skyt PS, Hil R, Booth JT. FlexyDos3D: a deformable anthropomorphic 3D radiation dosimeter: radiation properties. Phys Med Biol 2015;60(4):1543–63. https://doi.org/10.1088/0031-9155/60/4/1543.

[15] Høye EM, Sadel M, Kaplan L, Skyt PS, Muren LP, Petersen JBB, et al. First 3D measurements of proton beams in a deformable silicone-based dosimeter. J Phys Conf Ser 2017;847:012021. https://doi.org/10.1088/1742-6596/847/1/012021.

[16] Høye EM, Skyt PS, Balling P, Muren LP, Taasti VT, Swakoń J, et al. Chemically tuned linear energy transfer dependent quenching in a deformable, radiochromic 3D dosimeter. Phys Med Biol 2017;62(4):N73–89. https://doi.org/10.1088/1361-6560/aa512a.

[17] Høye EM. Towards clinical implementation of 3D dosimetry for intensity-modulated proton therapy. PhD thesis. Aarhus University; 2017.

[18] Feldkamp LA, Davis LC, Kress JW. Practical cone-beam algorithm. J Opt Soc Am A 1984;1(6):612. https://doi.org/10.1364/JOSAA.1.000612.

[19] Perl J, Shin J, Schümann J, Faddegon B, Paganetti H. TOPAS: An innovative proton Monte Carlo platform for research and clinical applications: TOPAS: An innovative proton Monte Carlo platform. Med Phys 2012;39(11):6818–37. https://doi.org/10.1118/1.4758060.

[20] Valdetaro L, Høye E-M, Skyt PS, Petersen JBB, Balling P, Muren LP. Empirical Linear-Energy-Transfer-based quenching correction in radiochromic 3D dosimetry of spot-scanning proton therapy (manuscript in preparation). Phys Imag. Radiat Oncol 2020.

[21] Low DA, Harms WB, Mutic S, Purdy JA. A technique for the quantitative evaluation of dose distributions. Med Phys 1998;25(5):656–61. https://doi.org/10.1118/1.598248.

[22] Maynard E, Heath E, Hilts M, Jirasek A. Evaluation of an x-ray CT polymer gel dosimetry system in the measurement of deformed dose. Biomed Phys Eng Express 2020;6:035031. https://doi.org/10.1088/2057-1976/ab895a.

[23] Rigaud B, Simon A, Castelli J, Lafond C, Acosta O, Haigron P, et al. Deformable image registration for radiation therapy: principle, methods, applications and evaluation. Acta Oncol 2019;58(9):1225–37. https://doi.org/10.1080/0284186X.2019.1620331.

[24] Chetty IJ, Rosu-Bubulac M. Deformable Registration for Dose Accumulation. Sem Radiat Oncol 2019;29(3):198–208. https://doi.org/10.1016/j.semradonc.2019.02.002.